Shear-Induced Micellar Structures in Ternary Surfactant Mixtures: The Influence of the Structure of the Micellar Interface

S. Hofmann

Bayer AG, Zentrale Forschung-Physik Disperser Systeme, E 41, 51368 Leverkusen, Germany

H. Hoffmann*

Universität Bayreuth, Physikalische Chemie I, 95440 Bayreuth, Germany

Received: November 26, 1997; In Final Form: February 25, 1998

New results are presented on the influence of the structure of surfactant headgroups on the ability of micelles to form shear-induced structures (SIS). Flow birefringence and electric birefringence results are reported on surfactant solutions of alkyldimethylamine oxide (C_{14}DMAO) and sodium dodecyl sulfate (SDS) and on solutions in which some of the C_{14}DMAO was substituted by $C_{12}E_6$ and the SDS by $C_{12}E_{2.5}SO_4Na$, respectively. In the mixed solutions of C_{14}DMAO and SDS, small rodlike micelles are present that show the electric birefringence anomaly. A second process appears in the electric birefringence signal that opposes the first one. The process is observed around the overlap concentration of the rodlike micelles. Under shear, solutions that give rise to the electric birefringence anomaly show anomalous flow behavior. For shear rates $\dot{\gamma}$ above a critical shear rate $\dot{\gamma}_c$, the solutions show the phenomenon of shear-induced structure formation. The solutions are shear-thickening for $\dot{\gamma} > \dot{\gamma}_c$. The flow birefringence results show that for $\dot{\gamma} > \dot{\gamma}_c$ a fraction of the micelles is completely aligned in the direction of flow. The SIS disappears with increased substitution of C_{14}DMAO by $C_{12}E_6$ and of SDS by $C_{12}E_{2.5}SO_4Na$, while the electric birefringence anomaly does not disappear. It is therefore concluded that the SIS formation is related to adhesive contacts between micelles.

1. Introduction

Since the early reports of Gravsholt,[1] it has been known that dilute solutions of certain ionic surfactants in which rodlike micelles are present give rise to an unusual rheological behavior if they are exposed to shear flow. This phenomenon had become the subject of many investigations. The phenomenon is both of principle and of practical scientific interest, because many of the surfactant solutions that show this phenomenon are able to reduce drag in turbulent pipe flow. The rodlike micelles that are present in dilute solutions of many surfactants rearrange under shear to form supramicellar structures (SIS) if a certain critical shear rate $\dot{\gamma}_c$ or critical shear stress is exceeded. These supramicellar structures are responsible for the anomalous flow behavior and for the drag reduction effect.[2−4] The characteristic conditions for SIS can be described as follows: Small, charged rodlike micelles well below or close to the overlap concentration c^* are present and rotate freely in the isotropic, low-viscosity quiescent solutions. If exposed to low shear rates, this situation remains unchanged until the critical shear rate $\dot{\gamma}_c$ is exceeded. Then the solutions show an increase in viscosity, a larger normal stress difference, and flow birefringence. In the course of early investigations on various surfactant systems (cetylpyridinium bromide/sodium salicylate, tetradecyltrimethylammonium bromide/sodium salicylate, hexadecyloctyldimethylammonium bromide $C_{16}C_8$DMABr), it could be shown by flow birefringence[5−7] and SANS experiments[8−10] that if the threshold value $\dot{\gamma}_c$ is passed a fraction of the micelles is completely aligned into the direction of flow. This alignment cannot be the result of simple hydrodynamic orientation since the product of $\dot{\gamma}_c$ and the rotational diffusion time τ_{rot} of a single micelle is always much less than unity. Therefore, a cooperative process plays an important role. After the shear is stopped, viscosity, normal stress difference, and birefringence relax with a certain time constant τ_s that is much longer than τ_{rot}. In most situations, during this relaxation process the SIS remains aligned in the direction of flow, indicating a disintegration process of the SIS rather than randomization of the SIS. It has been shown[7,11,12] that even after the solution has become isotropic again there are still some residual structures left that indicate that the SIS can be metastable for some time. The buildup and decay of SIS is also correlated with dynamic processes τ_{break} in micellar solutions. Addition of pentanol, for example, speeds up the dynamics and thus strongly affects the threshold value $\dot{\gamma}_c$.[2,7,13]

On the basis of these early results, Hoffmann and Rehage proposed a model in which the shear rate plays the role of an intrinsic thermodynamic variable[7] and triggers a process of micellar coagulation. An association equilibrium between micelles is shifted to the aggregation side by shear. In this way, long necklace-type aggregates are formed that become completely aligned in the direction of flow (pearl string model). In recent years Hu, Wang, and Matthys et al. also investigated the formation and decomposition of SIS.[12,14−18] Their results also support the view that a kinetic coagulation process takes place. SANS investigations of Kalus and Hoffmann indicated the formation of liquid crystalline structures under shear in surfactant solutions close to or above the micellar overlap concentration and provided the basis to regard SIS formation as a shear-induced transition to a nematic or hexagonal phase (phase transition model). New investigations of the Metz group and other authors on surfactant solutions—again above the overlap concentration ($c > c^*$)—provided strong evidence that a shear-

S1089-5647(98)00339-3 CCC: $15.00
Published on Web 06/25/1998

triggered switch from an isotropic viscoelastic state to an anisotropic (nematic) phase does indeed occur. A shear banding structure appeared and a two-phase region was observed when CTAB/NaSal solutions ($c > c^*$) were subjected to shear flow.[19−25]. The possibility of isotropic/liquid crystalline phase transitions under shear had been predicted theoretically by Marques, Cates, and See previously.[26,27] Very recently, a similar observation was made by Boltenhagen et al.[28] and Penfold et al.[29] with different surfactant systems. Both authors report the formation of ordered layers of surfactant aggregates in a shear-induced state starting from the walls of a shear cell and extending into the bulk of the solution with time.

However, it shall be pointed out that both models represent different points of view of one and the same process and do not need to be contradictory. Growth of micelles by coagulation and surfactant rearrangement to very long aggregates in dilute solutions is the prerequisite for SIS formation and implies no statement regarding the nature of the final structure after orientation in concentrated solutions. There are many experimental results that support both points of view.

Theoretical Considerations on Shear-Induced Surfactant Structures. Recent theoretical work follows three different approaches to explain the occurrence of the shear-thickening state. Bruinsma, Gelbart, and Ben-Shaul[30] consider that shear-enhanced collisions of rigid, rodlike micelles in the dilute state ($c < c^*$) lead to an aggregation of micelles, competing with a dissociation process induced by shear forces. They define a dimensionless Peclet number $P = \dot{\gamma}\cdot\tau_{rot}$ and a dimensionless concentration $C^* = c_t\cdot L^3$. Therefore, both parameters depend strongly on the length of the micellar aggregates (τ_{rot} = rotational relaxation time of a (super)micellar aggregate; c_t = particle concentration; L = length of a single micelle, micellar dimers, trimers, etc.). For $P < 1$ and $C^* < 1$, the system is in its equilibrium phase. The most decisive parameter is thus the resulting effective length of an aggregate. If $\dot{\gamma} \approx \dot{\gamma}_c$, the association rate exceeds the dissociation process and micellar oligomers are formed. The longer aggregates offer a larger cross section and lead to an increased collision rate. A positive feedback loop comes up. The process soon becomes catastrophical, and a percolation-like situation evolves leading to a network-like state, which could very well explain the viscoelastic properties of SIS (e.g., especially the overshoot of stress and birefringence at $\dot{\gamma} \geq \dot{\gamma}_c$) and the appearance of the "type 1" micelles (Kalus et al.[8−10]), which may be responsible for the short relaxation process of σ and Δn (in contrast to the fully aligned "infinitely" long micelles of the SIS that were termed "type 2" by the Kalus group and linked to the much longer relaxation times of SIS). Furthermore, as P and C^* both depend strongly on L, the system would automatically run into a situation where P and $C^* > 1$ and a gelation state would occur. This theory, like all others, does not include intermicellar interactions, which are doubtlessly important, but decouples the initial process of SIS formation from the subsequent alignment. It only discusses the triggering of the gelation. The two processes—gelation and alignment—are regarded as independent (and possibly of different physical origin).

In another approach, Wang[31−33] has developed a nonequilibrium thermodynamic theory in which growth and alignment is a means of reducing the tension and elastic energy stored in a sheared micelle. Rodlike micelles are subjected to considerable elastic forces when a shear field is applied. The micelles store the elastic energy like a Hooke'ian spring. Above a certain shear rate this deformation energy becomes so high that the micelles finally minimize their energy content by growth and alignment. The thermodynamics of self-assembly of micelles are compared with the elastic energy of scission in shear flow and finally coupled with the equation of shear rate dependent rotational diffusion. Wang's theory does not consider collisions (the importance of which he showed in his experimental work) and intermicellar interactions but leads to scaling laws that are very similar to those obtained by Bruinsma et al.

Finally, Cates[34,35] described the development of SIS in elongational flow. His approach describes both micellar growth and flow alignment by a collision process. According to his theory, only collinear collisions lead to association via the endcaps. The longer micelles become more and more aligned in shear flow, which increases the possibility of another successful collinear hit. Again a positive feedback loop is observed. The growth of the supermicellar aggregates is limited by the shear tension that leads to an increased breaking of the elongated micelles until an equilibrium state of gelation is observed. Cates confines his theory to elongational flow fields and states that SIS development in shear fields has to be supported by an additional cooperative process of interaction that accounts for the regime where $\dot{\gamma}_c\cdot\tau_{rot} \ll 1$. Again the obtained scaling laws coincide well with those of the other theories mentioned above.

In the first section (section 3.1), we review our previous work on mixed surfactant systems. Results of transient electric birefringence (TEB) measurements are used to check the state of micellar interaction in the quiescent solutions. In the following sections (sections 3.2−3.5), we then present new results on ternary surfactant mixtures that provide convincing evidence for the coagulation process.

2. Materials

1. The zwitterionic surfactants tetradecyldimethylamine oxide (C_{14}DMAO) and dodecyldimethylamine oxide (C_{12}DMAO) were a gift of the Hoechst AG, Gendorf. They were both purified by freeze-drying and two times recrystallization from acetone p.A. (Merck & Co.).

2. Sodium dodecyl sulfate (SDS) was bought from Serva (Heidelberg) as "SDS cryst. reinst" and used without further purification.

3. Hexaethylene glycol monododecyl ether ($C_{12}E_6$) was bought from NIKKO Chemical Co. Ltd., Tokyo, as a pure substance (GC).

4. The sodium alkyl ether sulfate $C_nE_{2.5}OSO_3Na$ was again a gift of Hoechst AG (Gendorf) (tradename "GENAPOL LRO") and received as an aqueous solution containing 27 wt % of surfactant (M_W = 382 g/mol). The technical product consists of a mixture of surfactants with 0−8 ethylene oxide units (number average 2.5) and a chain length distribution "n" of 75% C_{12} and 25% C_{14}. It was used without further purification.

3. Experiments

3.1. Flow and Electric Birefringence Studies on SIS and Micellar Interaction in a Binary Surfactant Mixture C_{14}DMAO/SDS. After it was realized that the charge of the micelles plays an important role in the formation of SIS, experiments were started with mixed nonionic/anionic surfactant systems. After the nearly ideal miscibility of C_{14}DMAO and SDS was proven,[36] we varied the mixing ratio of the two surfactants. It was thus possible to alter the micellar structure, the surface charge of the micelles, and, as a consequence, the micellar interaction to study the effect of these properties on SIS development. The aim was to find out which conditions a micellar solution must fulfill in order to be able to form SIS.

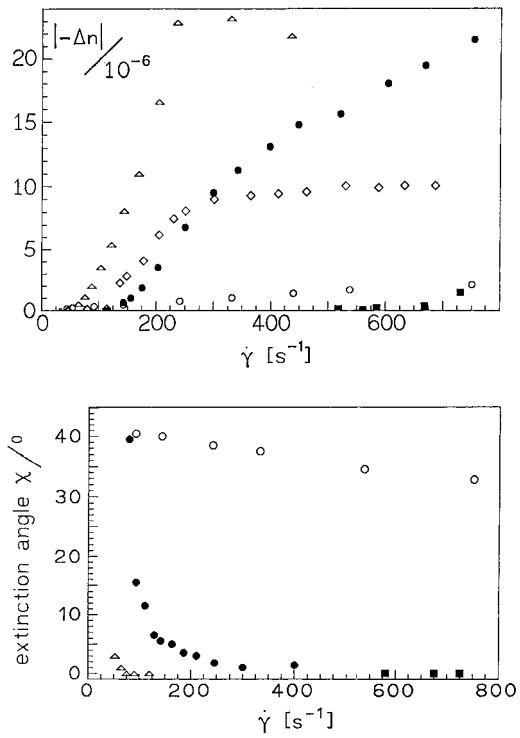

Figure 1. (a, top) Absolute flow birefringence $|-\Delta n|$ as a function of the shear rate for 100 mM solutions of C_{14}DMAO + SDS with different mixing ratios x = C_{14}DMAO:SDS (○, x = 9:1; ●, x = 8:2; △, x = 7:3; ◇, x = 6:4; ■, x = 5:5). (b, bottom) Extinction angle χ as a function of the shear rate for 100 mM solutions of C_{14}DMAO + SDS with different mixing ratios x = C_{14}DMAO:SDS (○, x = 9:1; ●, x = 8:2; △, x = 7:3; ■, x = 5:5).

The early experiments with the system C_{14}DMAO/SDS/H_2O focused on flow birefringence and rheological experiments with solutions of different mixing ratio, concentration, and salt content. The results have already been published.[37] Some of the results will be summarized here.

In addition to rheology, flow birefringence is a most appropriate tool to study shear-induced behavior of micellar systems. This method detects the average degree of orientation of unisometric aggregates as a function of the applied shear rate. In concentrated solutions of rodlike or wormlike micelles at $c > c^*$, the micelles overlap to form a network-like structure in the solution, which causes viscoelastic behavior. If shear is applied, this network is deformed and the solutions show birefringence. The intensity of birefringence $|\Delta n|$ increases linearly with shear rate while the extinction angle χ, which describes the average orientation of the unisometric aggregates (more exactly, their optical main axis) in reference to the direction of flow, is reduced slowly from a value close to 45° to a smaller one according to the law of Peterlin and Stuart. In case of total alignment into the direction of flow, χ approaches 0°. If, however, solutions of small rodlike micelles form SIS, the situation is different. At concentrations below the overlap concentration c^* and shear rates less than the critical shear rate $\dot{\gamma}_c$, the micelles are not aligned by flow and the solutions remain isotropic. No birefringence is detected at all. However, if $\dot{\gamma}_c$ is exceeded, birefringence is observed suddenly and increases toward a saturation value within a small interval of shear rate. Once formed, the SIS micelles are completely aligned toward the direction of flow ($\chi \rightarrow 0°$).

Solutions (100 mM) of mixtures of C_{14}DMAO and SDS at different mixing ratios give an example of both types of behavior. Figure 1a shows the flow birefringence of 100 mM solutions with different mixing ratios C_{14}DMAO/SDS and Figure 1b the corresponding course of the extinction angle versus the shear rate. The solution with the mixing ratio 9:1 shows a linear increase of Δn versus $\dot{\gamma}$ and a smooth drop of the extinction angle with increasing shear rate, the typical behavior of viscoelastic solutions of overlapping micelles in flow birefringence experiments (the individual micelles are too short to become oriented solely by hydrodynamics). All other mixing ratios shown in Figure 1a give rise to the characteristic S-shaped curves of the $|\Delta n|-(\dot{\gamma})$ plots. The critical shear rate has a minimum value at the ratio 7:3, and the plateau value $|\Delta n_{max}|$ becomes smaller with increasing content of SDS. The solution with a ratio of 5:5 exhibits a second critical shear rate $\dot{\gamma}_{c2}$ at 3200 1/s (not shown in Figure 1) above which the SIS is destroyed and the solution becomes isotropic again. Solutions of the mixing ratio 4:6 are no longer able to form SIS and remain isotropic over the whole accessible range of shear.

TABLE 1: Length of the Micelles in Comparison with Their Mean Mass Center Distances for 100 mM Solutions of Different Mixing Ratio (T = 25 °C)[a]

mixing ratio C_{14}DMAO:SDS	d (Å)	L (Å)
9:1	240 ± 20	>350
8:2[b]	190 ± 15	189 ± 40
7:3[b]	170 ± 10	130 ± 15
6:4[b]	160 ± 10	107 ± 15
5:5[b]	150 ± 10	103 ± 20
4:6	145 ± 10	95 ± 15

[a] The values were calculated by a combination of SANS and electric birefringence data.[37,38] The micelles were assumed to be of rodlike shape. The results of a detailed investigation of the micellar structures and a thorough, more exact evaluation of their dimensions have been published elsewhere.[36] [b] The mixing ratios at which the solutions develop SIS.

For this binary surfactant system, the flow birefringence behavior could be correlated with data on micellar dimensions and solution structure. The mean distance between the micelles and the length of the micelles that were assumed to be of cylindrical shape are given in Table 1. Both values were obtained by a combination of SANS and electric birefringence data.[37,38] Another and more detailed SANS study of the shape and dimensions of this mixed surfactant system has been published elsewhere.[36] Comparison of the data of Table 1 and Figure 1 makes it clear that SIS behavior is observed preferentially in the concentration regime below the overlap concentration c^*. The mixing ratios C_{14}DMAO:SDS = 5:5, 6:4, 7:3, 8:2 ($d \geq L$, cf. Table 1) reveal the S-shaped $|\Delta n|-(\dot{\gamma})$ plots of SIS, while 9:1 ($d < L$) shows the linear viscoelastic type increase of $|\Delta n|$ vs $\dot{\gamma}$. (However, additional investigations of the authors on this and different surfactant systems as well as studies of other researchers have shown that usually there is also a small concentration regime beyond c^* in which a superposition of both viscoelastic and shear-induced behavior is observed.)

Also, charge plays a major role in SIS formation. At C_{14}DMAO:SDS = 4:6 (60% ionic surfactant), the system is no longer able to form SIS although the micelles are still unisometric and $d > L$ (cf. Table 1). Furthermore, investigations on the dependence of $\dot{\gamma}_c$ on ionic strength I of the solutions revealed that $\dot{\gamma}_c \sim 1/\sqrt{I}$, which indicates the important role that surface charge and the electric double layers play for the formation of SIS.[37] It is also well-known that the binding of hydrophobic counterions to the micellar surface promotes the ability to form SIS. Combining these results it was concluded that the important parameters of SIS formation, $\dot{\gamma}_c$, Δn_{max}, and T_{ind}, are determined by a combination of micellar surface charge effects

(which include the effect of organic counterions and the influence of added salt) and structure parameters such as length and mean distance of the unisometric micelles.

It has been said before that the SIS-forming behavior of C_{14}-DMAO/SDS has been correlated to SANS and electric birefringence (EDB) data. It is important to note that the shape of the electric birefringence signals is a universal indicator of the state of the micellar solutions if charged rodlike micelles are present. Once data of micellar structure have been obtained by direct measurement (e.g., SANS, PCS, X-ray scattering) and a correlation with EDB-signal shape has been established, one can use the change of the signal shape to check the *relative* change of the state of micellar interaction and, consequently, to observe whether micelles become shorter or longer if a parameter (e.g., concentration, mixing ratio, salt content) is altered. EDB is of considerable advantage since the experiments are easy to perform and not time-consuming. In the subsequent step, one can refer this change of solution structure to the behavior in flow birefringence experiments and draw conclusions on SIS formation.

This was the experimental route we followed to obtain new information on SIS, which we report in this paper. Because of its importance, the structure of EDB signals and its correlation to micellar solution structure shall be described in the next section.

Electric birefringence effects in surfactant solutions have been reported in detail before.[39−41] Unisometric particles, such as rodlike micelles, can be aligned in an electric field, thereby giving rise to birefringence. The time-dependent response to pulsed electric fields (transient electric birefringence, TEB) or dynamic electric fields (DEB) provides valuable information: characteristic time constants of micellar dynamics can be derived from the buildup and decay of the signal. Buildup and decay of birefringence in solutions of charged, rodlike micelles are characterized by four time constants. In dilute solutions ($c \ll c^*$) far below the overlap concentration c^* only the fastest process is observed. It corresponds to counterion displacement followed by orientation of the unisometric micellar aggregates in the direction of the electric field. The relevation of the rodlike micelles after cessation of the pulse usually proceeds with a one-exponential or biexponential time dependence ($\tau_1 \leq 10\ \mu$s, $\tau_1^* = 10-100\ \mu$s) from which the lengths of the micelles can be calculated. In the semidilute regime ($c \leq c^*$) where the counterion clouds penetrate each other or the particles themselves may just come into contact, dipole formation by counterion displacement along the micellar axis of an individual micelle is difficult because the dipole is now part of an interpenetrating network of the double layers. In this situation, in addition to the first process, a second process of birefringence of opposite sign is observed. This so-called "anomalous" effect of the electric birefringence is a valuable and powerful indicator to probe the intermicellar interaction between micelles. This "anomalous" effect can be interpreted in terms of a orientation process that aligns part of the micelles perpendicular to the external electric field. The effect is associated with a time constant τ_2 covering a range from 10 μs to 1 ms. A third effect τ_3 finally appears for concentrated solutions $c > c^*$ for which the sign of the induced birefringence coincides with that of the first process (second anomalous effect). Its relaxation time constants are usually 1 order of magnitude larger than τ_2. It is thought to be the consequence of the orientation of network-like domains. In this latter case, free rotation of individual micelles is no longer possible. By use of the first and second anomalous effect, it is possible to distinguish between the semidilute regime in which the electric double layers of the micelles partially penetrate each other and the electrostatic interaction forces become significant ($c \leq c^*$, first anomalous effect) and the concentrated state in which the rotational volumes of the micelles start to overlap ($c \geq c^*$, second anomalous effect). This interpretation of both anomalous effects has been proposed first by Hoffmann.[40] Other interpretations have also been given.[42,43] Cates[43] assumes for the τ_2 process the buildup and alignment of swarms of parallel-oriented correlated rods perpendicular to the electric field. The perpendicular alignment would explain the reversal of the sign of birefringence. At the same time single rods would still align parallel to the E-field and would be the origin of the remaining first birefringence effect and its fast τ_1 relaxation process. This model is convincing if one considers the fact that the anomalous effect occurs in the concentration regime in which the micellar double layers just start to interfere with each other. The effect becomes especially pronounced if small stiff rodlike micelles are present in the solution. The longer the micelles are, the smaller is the concentration range and interval of E-field strength in which this first anomalous effect can be observed,[38] because longer micelles can always bend, to a certain degree, into the direction of the E-field.

Typical electric birefringence results on our mixed binary surfactant system are given next. These results provide the basis on which the results with the new ternary systems will be discussed.

Figure 2 shows the development of the TEB signals for 100 mM solutions at various mixing ratios. The micelles become longer with increasing amine oxide content (cf. Table 1). At 6:4 we are still below the overlap concentration ($d > L$), and only a nearly rectangular signal of negative birefringence $\Delta n_1(-)$ with very short relaxation time constant $\tau_1 < 1\ \mu$s (which is below the limit of resolution in this case) appears (Figure 2a). At 70% C_{14}DMAO (Figure 2b) the first anomalous effect is visible and the positive birefringence $\Delta n_2(+)$ dominates the signal. The region of buildup and decay of both effects can be distinguished clearly. At 7.5:2.5 the first negative contribution to Δn can no longer be detected owing to the longer sweep time and duration of pulse. $\Delta n_1(-)$ only manifests itself in the relaxation process. The second positive contribution is superimposed by the appearance of the third, negative effect $\Delta n_3(-)$, which reduces the resulting birefringence almost to zero. However, the relaxation of the three processes that contribute to Δn is still clearly visible (Figure 2c). On further increasing the share of C_{14}DMAO to 80% (Figure 2d), the negative effect $\Delta n_3(-)$ dominates totally. Traces of $\Delta n_1(-)$ and $\Delta n_2(+)$ are still present in birefringence buildup, while their relaxation can be observed more distinctively. Note, 8:2 is the ratio where the mean distance between the micelles and micellar length L becomes almost equal (cf. Table 1). 9:1 (Figure 2e) represents the ratio where $L > d$ and only the third effect $\Delta n_3(-)$ is visible. The duration of pulse and sweep time has to be increased in order to saturate birefringence and to detect the decay of the signal completely. It requires more time to align micelles in a network-like situation because in addition to rotation there is also some translational movement of the micelles necessary in order to become oriented parallel to the external field. At 100% C_{14}DMAO (Figure 2f) only the first negative $\Delta n_1(-)$ effect is visible. This is due to the fact that the alignment is now caused only by dipole orientation of the amine oxide headgroups and subsequent rotational movement of micelles, which results in a deviation from the rectangular signal which is typical for short charged rodlike micelles.

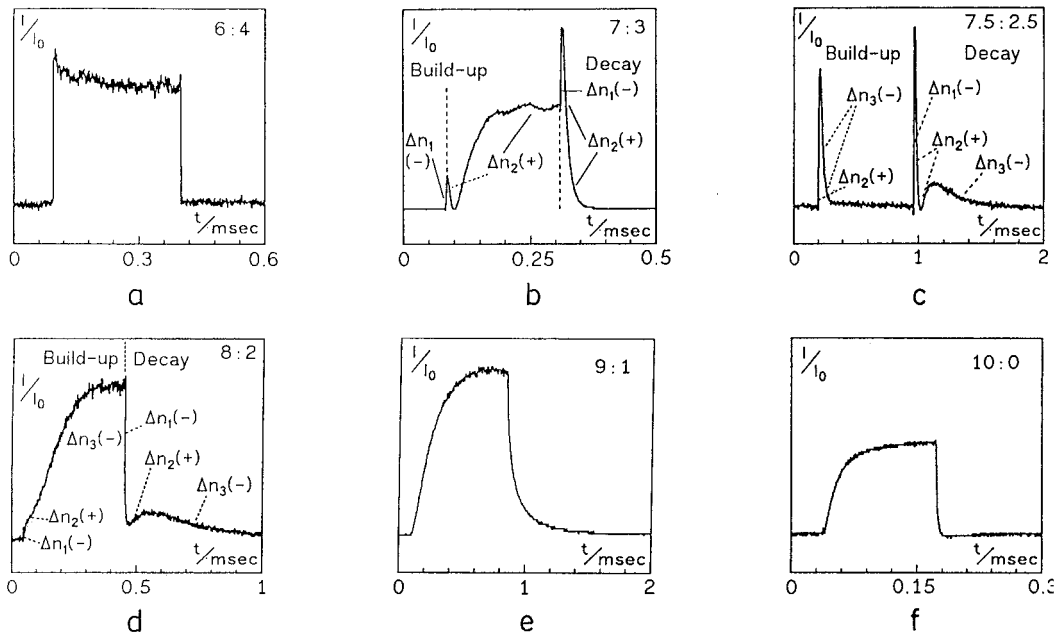

Figure 2. Transient electric birefringence signals for 100 mM solutions of C_{14}DMAO + SDS with increasing mixing ratios $x = C_{14}$DMAO:SDS at 25 °C and an electric field strength of 4×10^5 V/m (a, $x = 6{:}4$; b, $x = 7{:}3$; c, $x = 7.5{:}2.5$; d, $x = 8{:}2$; e, $x = 9{:}1$; f, $x = 10{:}0$) (note the different signs of the effects in b, c, and d).

Comparison with Figure 1 and Table 1 makes it evident that the ability of our surfactant system to form SIS can be correlated to the state of interaction at which $d \geq L$ and is represented by the rectangular signal ($d \gg L$) or the first anomalous effect ($d \geq L$) or the very first occurrence of the third effect ($d \approx L$) in EDB experiments. Therefore, once the standard has been set, any change in signal shape can be related to a change in micellar structure. For example, Figure 3 shows the shape of Δn signals with increasing concentration for a mixing ratio of C_{14}DMAO = 8:2. No exact SANS data on micellar dimensions are available for this composition, except for the 100 mM solution ($d \approx L$, Figure 3e). Note: Comparison with Figure 2d shows that the second positive effect $\Delta n_2(+)$ is now more marked, which is due to the smaller field strength used in this series. The occurrence of $\Delta n_2(+)$ is also dependent on field strength and pulse duration as it has been shown before.[39,44] Thus, to make use of the effect to detect relative changes in intermicellar interaction and micellar structure one has to find an appropriate range of field strength, pulse length, surfactant concentration, and, if needed, mixing ratio. This becomes more and more difficult the larger the micelles are.

On further addition of surfactant the length of the micelles must increase and finally exceed c^*. Consequently, at $c = 120$ mM (f) the third effect $\Delta n_3(-)$ dominates the response of the solution. On dilution at $c < 100$ mM, the micelles become smaller and therefore the third effect $\Delta n_3(-)$ is reduced (d, 90 mM) and the second effect $\Delta n_2(+)$ is fully developed (c, 80 mM). At 60 mM only a small part of birefringence is due to the second effect, and the rectangular signal of $\Delta n_1(-)$ is left at 50 mM where the solution is in the dilute state again (a, $c \ll c^*$). At the mixing ratio 8:2, solutions of $c > 120$ mM behave predominantly viscoelastic and no indication of SIS has been observed (birefringence data are not shown).

3.2. New Studies on the Mechanism of SIS Formation. To obtain a better understanding what kind of interaction is responsible for the formation of the SIS, the micellar surface was modified by introducing surfactants with spacer-like ethyleneoxide units into the micelles and by studying their effect on SIS formation. We substituted C_{14}DMAO partially by $C_{12}E_6$ or SDS by the technical surfactant $C_{12}E_{2.5}OSO_3Na$ (GENAPOL),

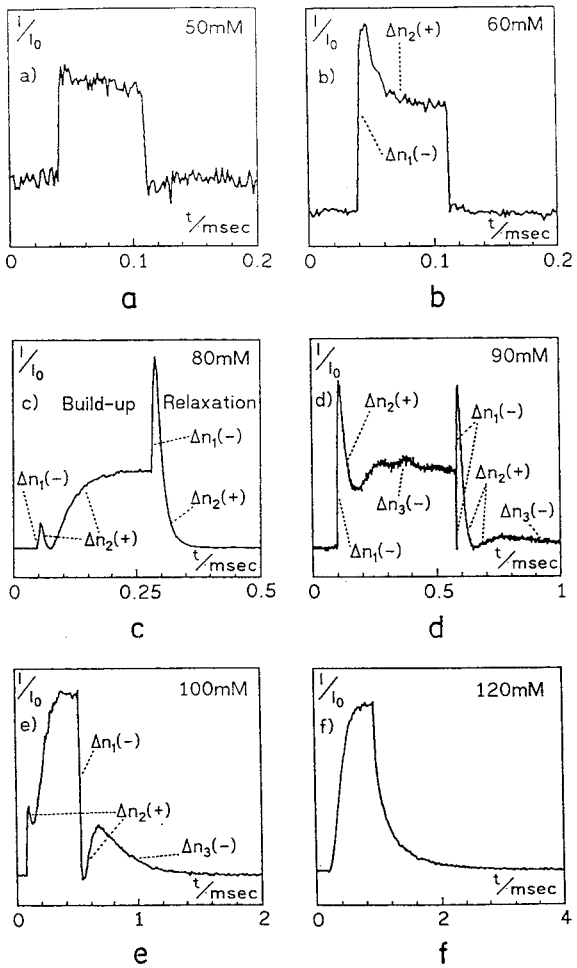

Figure 3. Transient electric birefringence signals for solutions of C_{14}-DMAO + SDS with a mixing ratio $x = 8{:}2$ and increasing total concentrations c at 25 °C and an electric field strength of 2×10^5 V/m (a, $c = 50$ mM; b, $c = 60$ mM; c, $c = 80$ mM; d, $c = 90$ mM; e, $c = 100$ mM; f, $c = 120$ mM).

here abbreviated as "GEN". We used TEB signals to detect the relative change of the micellar structures and interaction,

and subsequently we varied the total surfactant concentration to regain the original intensity of interaction of the binary system. To account for possible effects of the change of the micellar lifetime which becomes shorter if a surfactant with 13 CH_2 units is substituted by a surfactant with 11 CH_2 units, we repeated the experiment and substituted C_{14}DMAO partially by C_{12}DMAO. Therefore, we were able to separate the effects of the intensity of interaction and micellar kinetics from that of the structure of the micellar surface.

3.3. SIS Formation in the Ternary Surfactant System C_{14}DMAO/$C_{12}E_6$/SDS—Substitution of C_{14}DMAO by $C_{12}E_6$. To study the influence of the surfactant headgroup and the structure of the micellar surface on SIS, we substituted C_{14}-DMAO partially by $C_{12}E_6$ in a first series of experiments. We used $C_{12}E_6$ because its miscibility with C_{14}DMAO[45] and SDS[46] had been proven before and the area that the $C_{12}E_6$ headgroup requires at the micellar interface (32−47 Å^2, refs 47 and references cited therein and 45) is comparable to those of C_{14}-DMAO (42 Å^2, ref 48). Therefore, the structure of the micelles should not be altered too much if only a small amount of the amine oxide is substituted by $C_{12}E_6$. We took a mixing ratio C_{14}DMAO:SDS = 7:3 (c = 100 mM) and replaced the amine oxide stepwise: $x(C_{12}E_6) = n(C_{12}E_6)/[n(C_{12}E_6) + n(C_{14}DMAO)]$ = 0, 0.05, 0.1, 0.15, 0.2, 0.3. The change in the shape of the TEB signals (Figure 4) indicates that the micelles become increasingly smaller and the intensity of intermicellar interaction declines. The first anomalous effect of positive birefringence $\Delta n_2(+)$, which dominates the signal in the pure C_{14}DMAO/SDS solution, is continuously reduced and vanishes totally between $x(C_{12}E_6)$ = 0.2 and 0.3. Only the rectangular signal $\Delta n_1(-)$ caused by small rodlike micelles in the dilute state ($c < c^*$) remains. The absolute magnitude of birefringence and the relaxation time constants have also been evaluated but are omitted here because they provide no additional information in our context. The effect of the incorporation of the ethylene oxide surfactants on SIS formation is tremendous. The critical shear rate increases with increasing content of $C_{12}E_6$ (Figure 5). For x = 0.2, $\dot{\gamma}_c$ is about 1750 1/s and only a very weak birefringence is obtained. For x = 0.3, the solution remains isotropic up to $\dot{\gamma}$ = 3500 1/s and no trace of SIS can be observed. The upper limit of birefringence that can be detected by our apparatus is fixed by two effects: At $|\Delta n| \geq 15 \times 10^{-6}$ the polarized light is scattered by large supermicellar structures to such an extent that no compensation or even minimum of intensity could be reached by the Babinet compensation method. Second, the solutions start to foam if a certain shear rate, which depends on the mixing ratio, is reached and the beam of polarized light could not pass through the device any more. Therefore, the typical saturation effect of birefringence is not obtained here. (A detailed description of our flow birefringence apparatus and the detection method is given in ref 37 and references cited therein). The ability to form SIS is also lost if C_{14}DMAO is substituted by $C_{12}E_6$ in 100 mM solutions of other mixing ratios. (no figures shown). At 8:2, a 20% substitution of C_{14}DMAO by $C_{12}E_6$ is sufficient to suppress SIS formation and only a weak linear increase of $|\Delta n|$ with $\dot{\gamma}$ is observed. This viscoelastic effect is due to the fact that in 100 mM solutions of the mixing ratio 8:2 the micellar length becomes comparable to the mean mass center distance (cf. Table 1).

We then increased the total surfactant concentration of the solution with $x(C_{12}E_6)$ = 0.3 until the original intensity of interaction of the pure C_{14}DMAO/SDS solution was restored. This was again monitored by TEB (Figure 6). At c = 175 mM the shape of the original signal was obtained again, and at 200 mM c exceeds c^* as shown by the second anomalous effect $\Delta n_3(-)$. However, no restoration of the ability to build up SIS could be achieved. Instead, only viscoelastic behavior could be detected (i.e., constant increase of $|\Delta n|$ (Figure 7) and smooth decline of extinction angle with shear; data not shown). Therefore, incorporation of $C_{12}E_6$ into the micelles has completely destroyed the ability to form SIS.

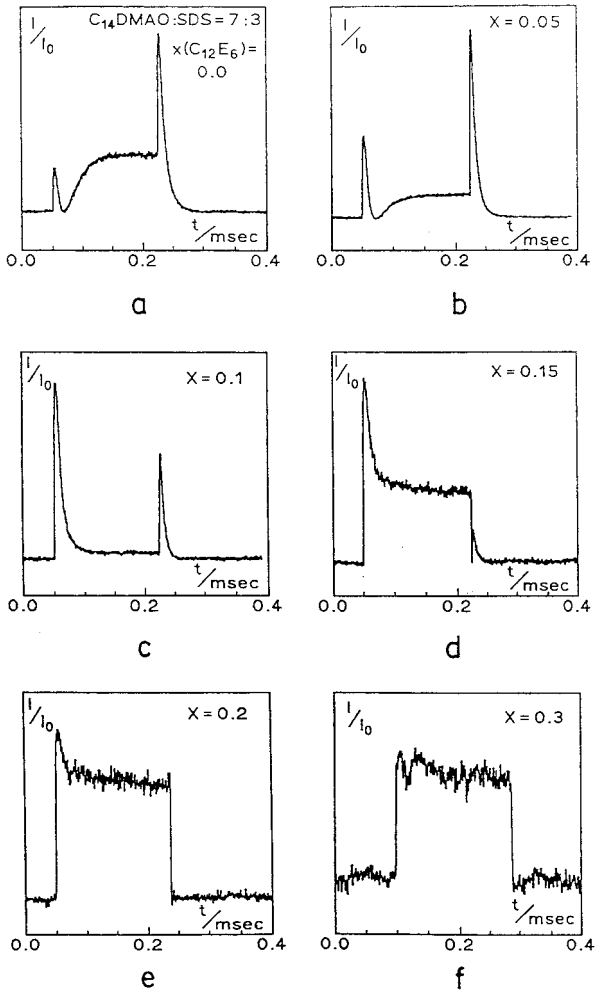

Figure 4. Transient electric birefringence signals for 100 mM solutions of (C_{14}DMAO + $C_{12}E_6$) + SDS with a mixing ratio x = (C_{14}DMAO + $C_{12}E_6$):SDS = 7:3 and increasing amounts of $x_{(C_{12}E_6)}$ ($x_{(C_{12}E_6)} = n_{(C_{12}E_6)}$:[$n_{(C_{12}E_6)} + n_{(C_{14}DMAO)}$]) at 25 °C and an electric field strength of 6 × 10^5 V/m (a, $x_{(C_{12}E_6)}$ = 0; b, $x_{(C_{12}E_6)}$ = 0.05; c, $x_{(C_{12}E_6)}$ = 0.1; d, $x_{(C_{12}E_6)}$ = 0.15; e, $x_{(C_{12}E_6)}$ = 0.2; f, $x_{(C_{12}E_6)}$ = 0.3).

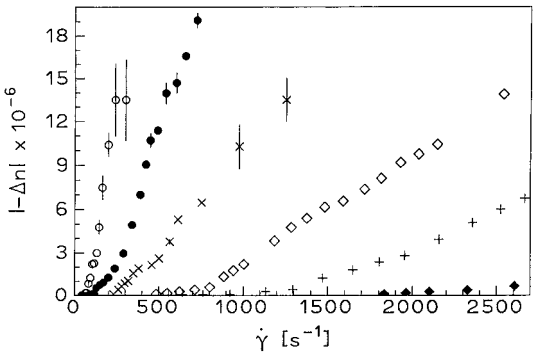

Figure 5. Absolute flow birefringence $|-\Delta n|$ as a function of the shear rate for 100 mM solutions of (C_{14}DMAO + $C_{12}E_6$) + SDS with a mixing ratio x = (C_{14}DMAO + $C_{12}E_6$):SDS = 7:3 and increasing amounts $x_{(C_{12}E_6)}$ ($x_{(C_{12}E_6)} = n_{(C_{12}E_6)}$:[$n_{(C_{12}E_6)} + n_{(C_{14}DMAO)}$]) (○, ($x_{(C_{12}E_6)}$ = 0; ●, $x_{(C_{12}E_6)}$ = 0.025; ×, $x_{(C_{12}E_6)}$ = 0.05; ◇, $x_{(C_{12}E_6)}$ = 0.1; +, $x_{(C_{12}E_6)}$ = 0.15; ◆, $x_{(C_{12}E_6)}$ = 0.2).

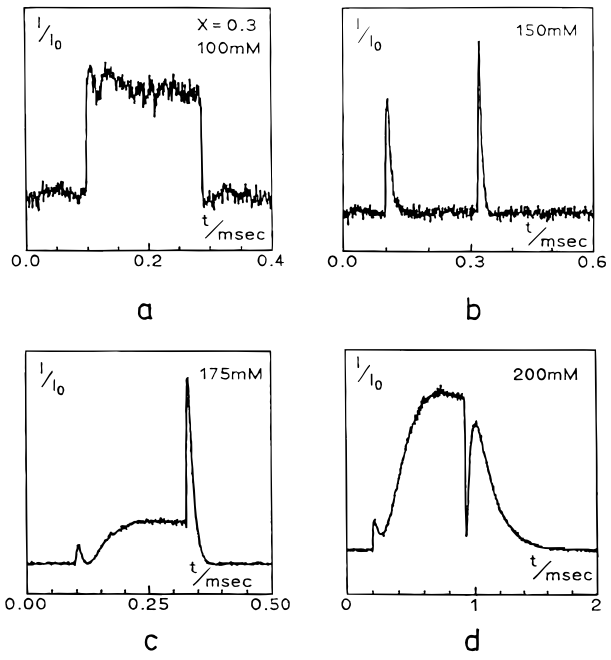

Figure 6. Transient electric birefringence signals for solutions of (C_{14}DMAO + $C_{12}E_6$) + SDS with a mixing ratio x = (C_{14}DMAO + $C_{12}E_6$):SDS = 7:3 and $x_{(C_{12}E_6)} = 0.3$ ($x_{(C_{12}E_6)} = n_{(C_{12}E_6)}$:[$n_{(C_{12}E_6)} + n_{(C_{14}DMAO)}$]) with different total concentrations c at 25 °C and an electric field strength of 6×10^5 V/m (a, c = 100 mM; b, c = 150 mM; c, c = 175 mM; d, c = 200 mM).

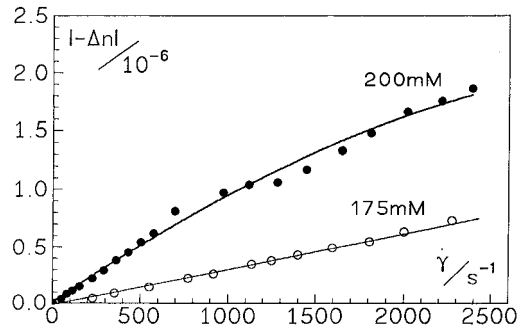

Figure 7. Absolute flow birefringence $|-\Delta n|$ as a function of the shear rate for 175 mM (○) and 200 mM (●) solutions of (C_{14}DMAO + $C_{12}E_6$) + SDS with a mixing ratio x = (C_{14}DMAO + $C_{12}E_6$):SDS = 7:3 and ($x_{(C_{12}E_6)} = 0.3$ ($x_{(C_{12}E_6)} = n_{(C_{12}E_6)}$:[$n_{(C_{12}E_6)} + n_{(C_{14}DMAO)}$]) at 25 °C.

3.4. SIS Formation in the Ternary Surfactant System C_{14}DMAO/SDS/GEN—Substitution of SDS by GENAPOL. In this second series of experiments we substituted SDS by the technical surfactant $C_{12}E_{2.5}OSO_3Na$, GENAPOL ("GEN"). On an average, 2.5 ethylene oxide units $-(CH_2CH_2O)-$ are inserted between the alkyl chain of an SDS molecule and its sulfate headgroup. This time we increased the amount of GEN until all of the SDS has been replaced by GEN: x(GEN) = n(GEN)/[n(GEN) + n(SDS) + n(C_{14}DMAO)] = 0, 0.05, 0.1, 0.15, 0.2, 0.3 (i.e., 0, 20, 33, 50, 66, 100% of SDS substituted by GEN).

We monitored the change in conductivity and pH when SDS was increasingly substituted by GEN. For comparison, we measured both properties also for other solutions of equal C_{14}DMAO/SDS and C_{14}DMAO/GEN mixing ratios. The results are given in Table 2. There is a clear tendency that the conductivity is reduced with increasing amounts of GEN. More interestingly, the pH values also become smaller. The high pH of about 11 of the original C_{14}DMAO/SDS solutions is a consequence of the mutual influence of the amine oxide and sulfate headgroups inside the micellar surface. The amine oxide molecules become partially protonated as the electronic state of the N−O dipole is influenced by the negative charge of the neighboring sulfate headgroups. The basic character of the N−O unit becomes stronger (pK_a of N−OH$^+$ greater) in the mixed micelles, a typical feature of synergism. Therefore the reduction of the pH with increasing addition of GEN is a strong indication that the contact between sulfate and amine oxide headgroups is less intensive than in C_{14}DMAO/SDS micelles, thus indicating the spacer-like function of the ethylene oxide units in GEN, which causes the sulfate headgroups to protrude from the micellar interface.

TABLE 2: Conductivity and pH Values of C_{14}DMAO/SDS/GEN Mixtures[a]

C_{14}DMAO:GEN:SDS			C_{14}DMAO			C_{14}DMAO		
7:x:(3 − x)	σ (mS)	pH	SDS	σ (mS)	pH	GEN	σ (mS)	pH
x = 0	7.25	11.01	8:2	5.41	10.63	8:2	4.95	10.25
x = 0.5	7.05	11.04	7:3	7.25	11.01	7:3	6.69	10.36
x = 1	6.82	10.68	6:4	9.2	11.17	6:4	8.0	10.33
x = 1.5	7.0	10.76	5:5	11.0	11.05	5:5	9.07	10.16
x = 2	7.12	10.87						
x = 3	6.69	10.36						

[a] The values with increasing replacement of SDS by GEN are given in the left column. In the other two columns, both properties are compared for the corresponding C_{14}DMAO/SDS and C_{14}DMAO/GEN molar ratios; c = 100 mM; T = 25 °C.

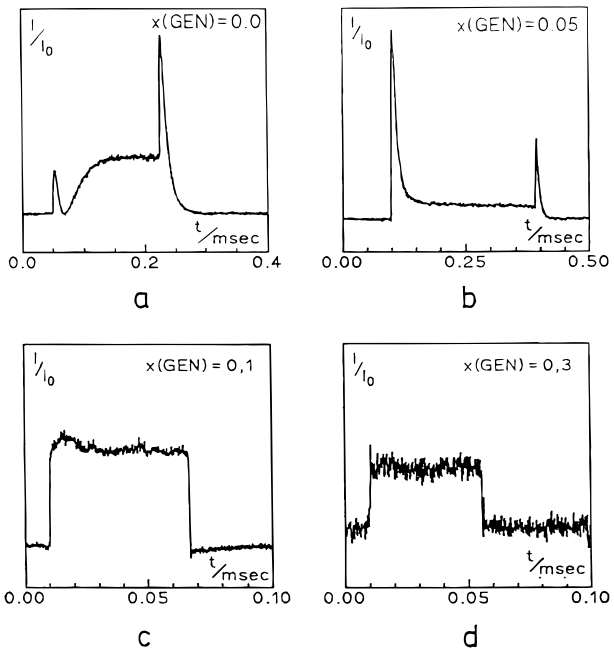

Figure 8. Transient electric birefringence signals for 100 mM solutions of C_{14}DMAO + (SDS + GEN) with a mixing ratio x = C_{14}DMAO:(SDS + GEN) = 7:3 and increasing amounts of x_{GEN} ($x_{GEN} = n_{GEN}$:[$n_{GEN} + n_{(C_{14}DMAO)} + n_{SDS}$]) at 25 °C and an electric field strength of 6×10^5 V/m (a, x_{GEN} = 0; *b*, x_{GEN} = 0.05; c, x_{GEN} = 0.1; d, x_{GEN} = 0.3).

The effect of this replacement on the scale and intensity of intermicellar interaction was observed by TEB again. Some signals of solutions of the composition C_{14}DMAO:(SDS + GEN) = 7:3 are shown in Figure 8 as an example. The micelles become shorter (overall birefringence $\Sigma|\Delta n|$ is reduced) and the anomalous effect disappears completely if 33% of SDS has been replaced (x(GEN) = 0.1). Figure 9 shows the consequence for SIS formation. The results are identical to those obtained by C_{14}DMAO/$C_{12}E_6$ exchange. After total replacement of SDS (x = 0.3), the solutions remain isotropic over the whole accessible shear range up to 3000 1/s. To be sure that there is

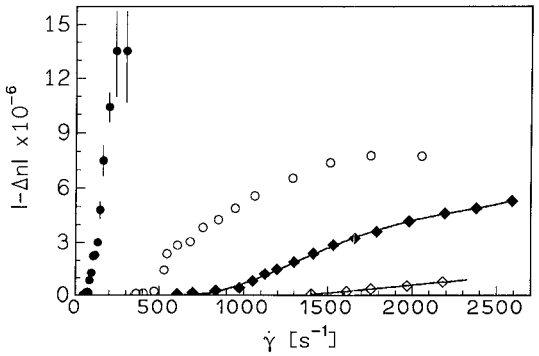

Figure 9. Absolute flow birefringence $|-\Delta n|$ as a function of the shear rate for 100 mM solutions of C_{14}DMAO + (SDS + GEN) with a mixing ratio $x = C_{14}$DMAO:(SDS + GEN) = 7:3 and increasing amounts of x_{GEN} ($x_{GEN} = n_{GEN}:[n_{GEN} + n_{(C_{14}DMAO)} + n_{SDS}]$) at 25 °C (●, $x_{GEN} = 0$; ○, $x_{GEN} = 0.1$; ◆, $x_{GEN} = 0.15$; ◇, $x_{GEN} = 0.2$) (the solution with $x_{GEN} = 0.3$ remains isotropic).

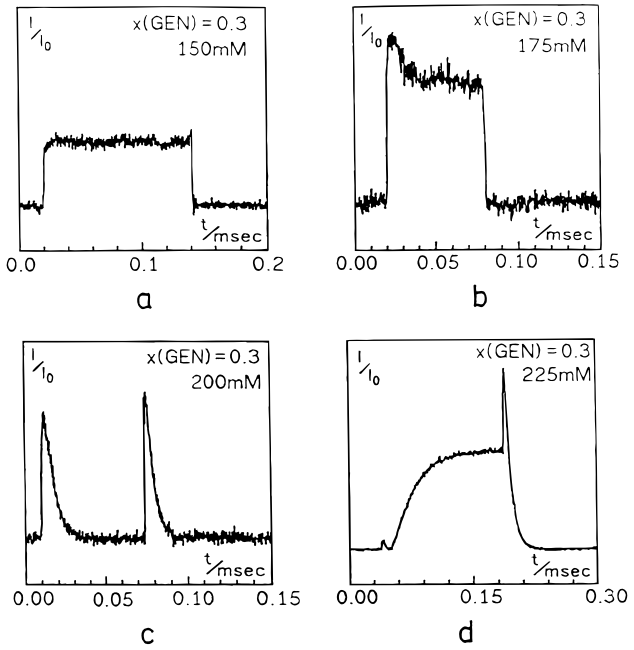

Figure 10. Transient electric birefringence signals for solutions of C_{14}-DMAO + (SDS + GEN) with a mixing ratio $x = C_{14}$DMAO:(SDS + GEN) = 7:3 and $x_{GEN} = 0.3$ ($x_{GEN} = n_{GEN}:[n_{GEN} + n_{(C_{14}DMAO)} + n_{SDS}]$) with different total concentrations c at 25 °C and an electric field strength of 6×10^5 V/m (a, $c = 150$ mM; b, $c = 175$ mM; c, $c = 200$ mM; d, $c = 225$ mM).

no SIS beyond 3000 1/s, up to 100 mM NaCl was added. If there was SIS above 3000 1/s, the salt would shift the critical shear rate to lower values. But even then the solution remained isotropic.

We then increased the total surfactant concentration of the solution with x(GEN) = 0.3. Figure 10 shows the shape of the TEB signals. At $c = 175$ mM the first anomalous effect Δn_2-(+) sets in; between 200 and 225 mM the original intensity of interaction is regained. But again only a linear increase of Δn and no trace of shear-induced behavior was found for the 200 and 225 mM solutions (Figure 11). As in the case of $C_{12}E_6$, the incorporation of the alkyl ether sulfate GENAPOL into the mixed micelles also inhibits the formation of SIS irreversibly.

3.5. SIS Formation in the Ternary Surfactant System C_{14}DMAO/C_{12}DMAO/SDS—Substitution of C_{14}DMAO by C_{12}DMAO. The formation of SIS is closely related to the mean micellar lifetime τ_{break}. It is evident that supermicellar structures can only be formed if τ_{break} is long enough to build up large

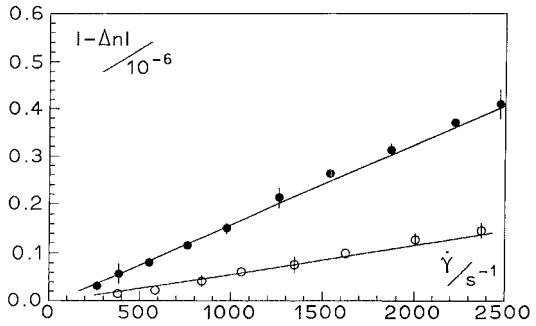

Figure 11. Absolute flow birefringence $|-\Delta n|$ as a function of the shear rate for 200 mM (○) and 225 mM (●) solutions of C_{14}DMAO + (SDS + GEN) with a mixing ratio $x = C_{14}$DMAO:(SDS + GEN) = 7:3 and $x_{GEN} = 0.3$ ($x_{GEN} = n_{GEN}:[n_{GEN} + n_{(C_{14}DMAO)} + n_{SDS}]$) at 25 °C (no presence of shear-induced structures).

structures. The condition $\dot{\gamma}_c \cdot \tau_{break} > 1$ has to be fulfilled. It is also evident that τ_{break} becomes shorter if surfactants with shorter hydrocarbon chains are incorporated into a micelle, because the energy that is needed to transfer, e.g., 11 CH_2 units from the micelle into the solvent is lower than the energy needed for 13 CH_2 units. Therefore, one could argue that by replacement of C_{14}DMAO by $C_{12}E_6$ τ_{break} is simply reduced to such an extent that the condition $\dot{\gamma}_c \cdot \tau_{break} > 1$ is no longer fulfilled.

To be sure that this is not the reason for the vanishing of SIS, we performed a third series of experiments in which we substituted C_{14}DMAO by C_{12}DMAO and studied the effects on SIS and the TEB signals. Six solutions with a mixing ratio (C_{14}DMAO + C_{12}DMAO):SDS = 7:3, $c = 100$ mM, and x(C_{12}-DMAO) = n(C_{12}DMAO)/[n(C_{14}DMAO) + n(C_{12}DMAO)] = 0, 0.1, 0.2, 0.3, 0.4, 0.6 were prepared. Figure 12 shows the effects on the TEB signals. As expected, the first anomalous effect $\Delta n_2(+)$ vanishes again and the stationary birefringence is reduced, which means that the micelles become shorter. At $x = 0.6$ only very short, more or less spheroidal, micelles exist, which is indicated by the remaining weak birefringence (-5.4×10^{-9} [38]). Figure 13 shows the effect on SIS formation. The solutions remain isotropic in the observed shear range if x(C_{12}-DMAO) ≥ 0.6. Increasing the total surfactant concentration reconstitutes the original intensity of micellar interaction by increasing the number density of the micelles (Figure 14). First $\Delta n_2(+)$ and second $\Delta n_3(-)$ anomalous effects reappear. In contrast to the first two series of experiments, the ability to form SIS is regained (Figure 15). The same effect is observed if an increasing amount of salt is added to the solution with x(C_{12}-DMAO) = 0.6 (Figure 16). In both series one can observe the transition from pure shear-induced to combined shear-induced/viscoelastic and finally pure viscoelastic behavior as is revealed by the course of the $|\Delta n|-(\dot{\gamma})$ plot.

4. Discussion

The experiments showed the dependence of SIS formation on the structure of the micellar interface. We introduced ethylene oxide units as a part of the surfactant headgroups into the rodlike micelle. By use of the anomalous effect in TEB experiments we kept the intensity of interaction constant by increasing the concentration. Despite this, the ability to form SIS was completely lost. The counter experiment of C_{14}DMAO substitution by C_{12}DMAO proved that the loss of this ability is not only due to a possible failure to fulfill the condition $\dot{\gamma}_c \cdot \tau_{break} > 1$ when C_{14}DMAO was partially replaced by $C_{12}E_6$. The important conclusion that must be drawn from these experiments is that the presence of rodlike micelles that carry a proper surface charge is a necessary but not sufficient condition for the

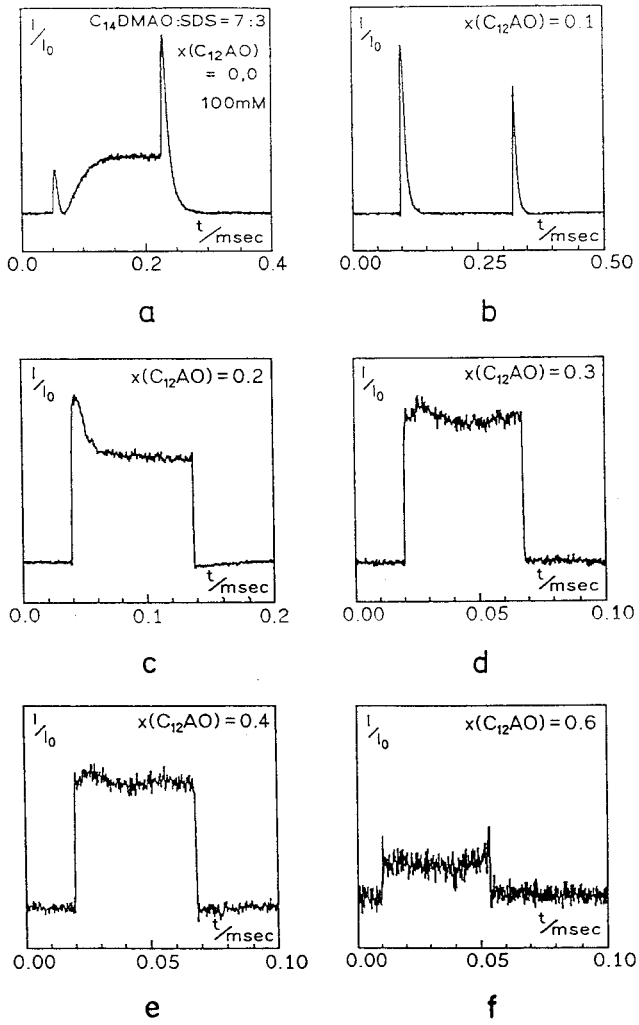

Figure 12. Transient electric birefringence signals for 100 mM solutions of (C_{12}DMAO + C_{14}DMAO) + SDS with a mixing ratio x = (C_{12}DMAO + C_{14}DMAO):SDS = 7:3 and increasing values of $x_{(C_{12}DMAO)}$ ($x_{(C_{12}DMAO)} = n_{(C_{12}DMAO)}$:[$n_{(C_{12}DMAO)} + n_{(C_{14}DMAO)}$]) with different total concentrations c at 25 °C and an electric field strength of 6×10^5 V/m (a, $x_{(C_{12}DMAO)} = 0$; b, $x_{(C_{12}DMAO)} = 0.1$; c, $x_{(C_{12}DMAO)} = 0.2$; d, $x_{(C_{12}DMAO)} = 0.3$; e, $x_{(C_{12}DMAO)} = 0.4$; f, $x_{(C_{12}DMAO)} = 0.6$).

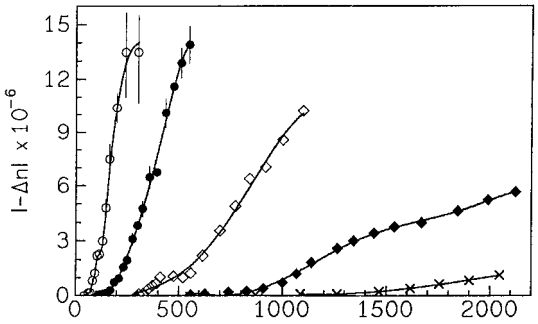

Figure 13. Absolute flow birefringence $|-\Delta n|$ as a function of the shear rate for 100 mM solutions of (C_{12}DMAO + C_{14}DMAO) + SDS with a mixing ratio x = (C_{12}DMAO + C_{14}DMAO):SDS = 7:3 and increasing values of $x_{(C_{12}DMAO)}$ ($x_{(C_{12}DMAO)} = n_{(C_{12}DMAO)}$:[$n_{(C_{12}DMAO)} + n_{(C_{14}DMAO)}$]) at 25 °C (○, $x_{(C_{12}DMAO)} = 0$; ●, $x_{(C_{12}DMAO)} = 0.1$; ◇, $x_{(C_{12}DMAO)} = 0.2$; ◆, $x_{(C_{12}DMAO)} = 0.3$; ×, $x_{(C_{12}DMAO)} = 0.4$; the solution with $x_{(C_{12}DMAO)} = 0.6$ remains isotropic).

formation of SIS. The type of headgroup seems to be a decisive parameter, too. It has been shown that the modification of the micellar surface structure by incorporation of ethoxy groups has a marked (and in this case devastating) effect on the capability of the micelles to develop SIS. The occurrence of the

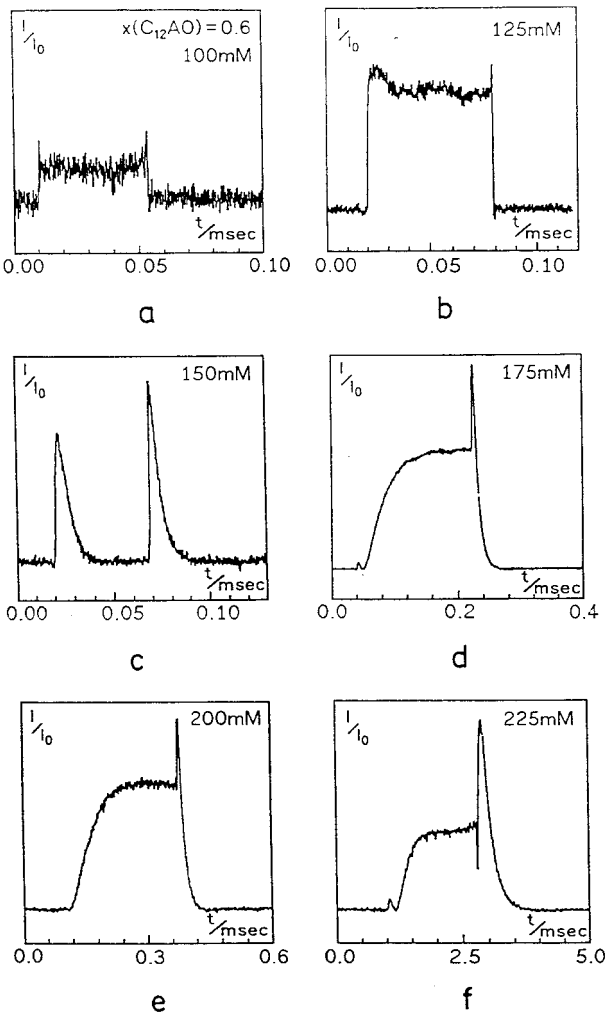

Figure 14. Transient electric birefringence signals for solutions of (C_{12}-DMAO + C_{14}DMAO) + SDS with a mixing ratio x = (C_{12}DMAO + C_{14}DMAO):SDS = 7:3 and $x_{(C_{12}DMAO)} = 0$ ($x_{(C_{12}DMAO)} = n_{(C_{12}DMAO)}$:[$n_{(C_{12}DMAO)} + n_{(C_{14}DMAO)}$]) with different total concentrations c at 25 °C and an electric field strength of 6×10^5 V/m (a, c = 100 mM; b, c = 125 mM; c, c = 150 mM; d, c = 175 mM; e, c = 200 mM; f, c = 225 mM).

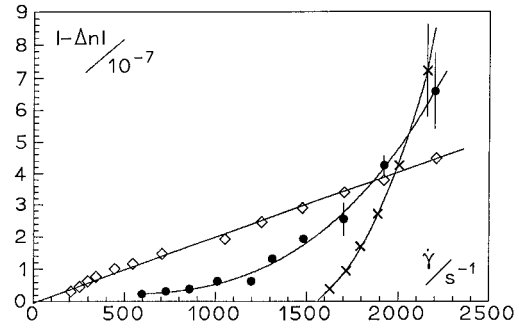

Figure 15. Absolute flow birefringence $|-\Delta n|$ as a function of the shear rate for solutions of (C_{12}DMAO + C_{14}DMAO) + SDS with a mixing ratio x = (C_{12}DMAO + C_{14}DMAO):SDS = 7:3 and $x_{(C_{12}DMAO)}$ = 0.6 ($x_{(C_{12}DMAO)} = n_{(C_{12}DMAO)}$:[$n_{(C_{12}DMAO)} + n_{(C_{14}DMAO)}$]) with different total concentrations c at 25 °C (×, c = 125 mM; ●, c = 150 mM; ◇, c = 175 mM).

supramolecular structure does not only depend on long-range electrostatic interaction but also on short-distance steric interaction. Although there is still no information available about the exact conformation of the $(EO)_x$ groups at the micellar surface, it is obvious that the protrusion of these groups from the micellar interface prevents the SIS formation. This is only possible if

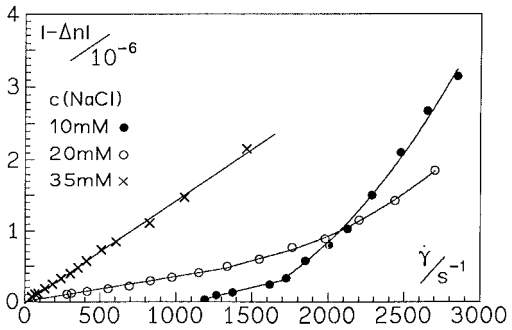

Figure 16. Absolute flow birefringence $|-\Delta n|$ as a function of the shear rate for 100 mM solutions of (C_{12}DMAO + C_{14}DMAO) + SDS with a mixing ratio x = (C_{12}DMAO + C_{14}DMAO):SDS = 7:3 and $x_{(C_{12}DMAO)} = 0.6$ ($x_{(C_{12}DMAO)} = n_{(C_{12}DMAO)}$:[$n_{(C_{12}DMAO)} + n_{(C_{14}DMAO)}$]) with increasing concentrations c_{NaCl} of NaCl at 25 °C (●, c_{NaCl} = 10 mM; ○, c_{NaCl} = 20 mM; ×, c_{NaCl} = 35 mM).

the micelles that take part in the shear-induced superstructure have to come very close to each other in order to form SIS. Therefore only the pearl-string or coagulation model is consistent with these new results. Not only long-range electrostatic interaction but also the microscopic properties of the micellar interface structure are important for SIS. This could also provide a better understanding why organic counterions that bind to the micellar interface promote SIS formation. Attached naphthoate or salicylate ions not only cause micelles to grow but also give rise to a short-distance hydrophobic interaction, which could make it more favorable for the micelles to stick together.

These results make it doubtful to interpret SIS formation exclusively as an isotropic to nematic phase transition as has been proposed before[37] and as it seems to be supported by results with concentrated solutions at $c > c^*$.[19−29] If the individual micelles of the isotropic state keep their integrity in SIS, it is difficult to understand why a simple modification of surface structure—while keeping the interaction forces constant—should prevent them from being arranged parallel to each other in a liquid crystalline phase. The view of SIS as a simple metastable (nematic) phase becomes more doubtful as the authors could show that the mixing ratios where the system C_{14}DMAO/SDS is able to form SIS (8:2−5:5) do not coincide with the existence range of nematic phases. The phase diagram of the binary system has been published before.[49] Although the system forms nematic phases at mixing ratios C_{14}DMAO:SDS of roughly 2:8−9:1—followed by hexagonal phase areas at higher concentrations—no SIS could be detected at mixing ratios of, e.g., 3:7, even if isotropic solutions close to the phase boundary have been subjected to a flow birefringence study. Only isotropic or viscoelastic behavior could be observed.

However, once again it shall be pointed out that the coagulation of micelles under the influence of shear is the starting point of SIS formation. Our experiments provide strong experimental evidence that a coagulation process is underlying the generation of supermicellar structures. But this includes no evidence about the nature of the fully developed aligned micelles in SIS.

Orientation and long-range order of SIS micelles could be regarded as a transition of the extremely long SIS aggregates in a gellike state to an energetically more favorable ordered and aligned state in order to ease their intense steric and electrostatic interaction when subjected to shear stress. As a consequence, the orientation process may not simply be described by the application of the simple or extended orientational distribution equation of rod axis under the influence of shear, which has been the basis of many experimental SANS and theoretical investigations (cf. Kalus et al.[50−52] and Wang et al.[31−33]). Instead it may be useful to describe the SIS generation by two independent processes: association to long and strongly (sterical and electrostatical) interacting wormlike micellar aggregates (cf. theory of Bruinsma, Gelbart, and Ben-Shaul[30]) and subsequent ordering under shear (a theoretical description would require the consideration of minimizing the energy content of the system and would have to include a shear rate dependent electrostatic interaction term coupled to the mutual orientation of the micelles). The separation of association and alignment would also account for the failure to describe the formation of SIS in dilute solutions ($c < c^*$, $\dot{\gamma}_c$ *decreases* with concentration) and semidiluted or concentrated solutions ($c > c^*$, $\dot{\gamma}_c$ *increases* with concentration) by one single theory.[53]

Conclusions

In the first part of the investigation flow and electric birefringence measurements are reported for aqueous micellar solutions of the mixed surfactants tetradecyldimethylamine oxide and sodium dodecyl sulfate. The combination of the two surfactants gives rise to a synergistic behavior which is reflected in the zero-shear viscosity η° of the mixtures. The viscosity η° for 100 mM solutions passes over a maximum with increasing mole fraction X_a of the anionic surfactant. The maximum occurs at $X_a \sim 0.1$. Solutions with $X_a \leq 0.1$ show a normal flow behavior and give rise to normal electric birefringence signals: The flow birefringence increases linearly with the shear rate, and the electric birefringence signal shows a single rise and decay process with a rectangular electric field pulse. Solutions with X_a between 0.2 and 0.5 show anomalous properties of the flow and the electric birefringence behavior. Under shear the solutions show the phenomenon that is known under the name of shear-induced structure (SIS) formation. The solutions do not show birefringence as long as the shear rate is smaller than a critical shear rate $\dot{\gamma}_c$ ($\dot{\gamma} < \dot{\gamma}_c$). For $\dot{\gamma} > \dot{\gamma}_c$, the flow birefringence increases abruptly and the extinction angle that is determined from the birefringence shows that a fraction of the micelles is completely aligned in the direction of flow. After the shear is stopped, the solutions relax back to the isotropic state. Electric birefringence measurements reveal three distinct processes in this concentration range. With increasing concentration and X_a between 0.2 and 0.6, one first observes a single process τ_1 that is due to the rotation of small rodlike micelles. The sign of the birefringence of this process is negative, and the rods align parallel to the electric field. For solutions in which the rods are around the overlap concentration c^*, a second process is observable with an opposite sign, that indicates that some of the rods are aligned perpendicular to the field. Finally for $c > c^*$ the two fast processes with τ_1 and τ_2 disappear and are replaced by a third process with a relaxation time τ_3 that is about a factor of 10 longer than τ_2. It is argued that the τ_2 process is due to the rotation of rodlike micelles that seem to have a permanent dipole perpendicular to the rod axis. Around the overlap concentration c^* all three processes are observed in one and the same solution. The combined results from the flow and electric birefringence data show that the product of $\dot{\gamma}_c$ and the rotation time constants for the rodlike micelles is much smaller than 1 ($\dot{\gamma} \cdot \tau_{rot} \ll 1$), which shows that the small rodlike micelles cannot be aligned by the hydrodynamic interaction of the shear.

In the second part results of electric birefringence and flow birefringence measurements of micellar solutions are presented for which the surface of the micelles had been modified by other

surfactants. Some of the alkylamine oxide in the micelles was replaced by the classic nonionic surfactant $C_{12}E_6$ or some of the SDS was replaced by an anionic dodecyl ethoxysulfate ($C_{12}E_{2.5}SO_4Na$). The results show that the rodlike micelles are decreasing somewhat in size by both substitutions. The same intermicellar interaction and the same electric birefringence signals can, however, be regained as in the case of the unsubstituted solution if the total surfactant concentration is increased. The flow birefringence data show, however, that the SIS formation is prevented with increasing substitution of the alkylamine oxide or the SDS by $C_{12}E_6$ and $C_{12}E_{2.5}SO_4Na$, respectively. It is therefore argued that the *protrusion* of the EO groups from the micellar surfaces suppresses the formation of the SIS. It seems, therefore, that SIS formation is related to adhesive forces between micellar surfaces. Without the protruding EO groups the small rodlike micelles from C_{14}DMAO and SDS can form adhesive contacts even though their interaction is repulsive.

Acknowledgment. Financial support of this work by the Deutsche Forschungsgemeinschaft (DFG) and the Sonderforschungsbereich SFB 213 is gratefully acknowledged.

References and Notes

(1) Gravsholt, S. *J. Colloid Interface Sci*. **1976**, *57* (3), 575−577; *Naturwissenschaften* **1979**, *66* (5), 363−264.
(2) Ohlendorf, D.; Interthal, W.; Hoffmann, H. *Rheol. Acta* **1986**, *25*, 468−486.
(3) Smith, B. C.; Chou, L.-C.; Lu, B.; Zakin, J. L. *ACS Symp. Ser.* **1994**, *578* (Structure and Flow in Surfactant Solutions), 370−379.
(4) Hofmann, S.; Stern, P.; Myska, J. *Rheol. Acta* **1994**, *33*, 419−430.
(5) Rehage, H.; Hoffmann, H. *Rheol. Acta* **1982**, *21*, 561−563.
(6) Rehage, H.; Wunderlich, I.; Hoffmann, H. *Prog. Colloid Polym. Sci*. **1986**, *72*, 51−59.
(7) Wunderlich, I.; Hoffmann, H.; Rehage, H. *Rheol. Acta* **1987**, *26*, 532−542.
(8) Kalus, J.; Hoffmann, H.; Ibel, K. *Colloid Polym. Sci.* **1989**, *267*, 818−824.
(9) Kalus, J.; Hoffmann, H.; Lindner, P. *Prog. Colloid Polym. Sci.* **1989**, *79*, 233−238.
(10) Jindal, V. K.; Kalus, J.; Pilsl, H.; Hoffmann, H.; Lindner, P. *J. Phys. Chem.* **1990**, *94*, 3129−3138.
(11) Prötzl, B. Ph.D. Thesis, 1996, TU Berlin. Prötzl, B.; Springer, J. *J. Colloid Interface Sci.* **1997**, *190*, 327−333.
(12) Hu, Y.; Wang, S.-Q.; Jamieson, A. M. *J. Rheol.* **1993**, *37* (3), 531−546.
(13) Makhloufi, R.; Decruppe, J. P.; Cressely, R. *Colloids Surf. A* **1993**, *76* (1−3), 33−39.
(14) Hu, Y.; Wang, S.-Q.; Jamieson, A. M. *J. Colloid Interface Sci.* **1993**, *156*, 31−37.
(15) Hu, Y.; Wang, S.-Q.; Rajamram, C. V.; Jamieson, A. M. *Langmuir* **1994**, *10*, 80−85.
(16) Hu, Y.; Matthys, E. F. *Rheol. Acta* **1995**, *34* (5), 450−460.
(17) Hu, Y.; Matthys, E. F. *Rheol. Acta* **1996**, *35* (5), 470−480.
(18) Hu, Y.; Matthys, E. F. *J. Rheol. (N. Y.)* **1997**, *41* (1), 151−166.
(19) Hartmann, V.; Cressely, R. *Colloids Surf. A* **1997**, *123* (2−3), 151−162.
(20) Cappelaere, E.; Berret, J. F.; Decruppe, J. P.; Cressely, R.; Lindner, P. *Phys. Rev. E* **1997**, *56* (2), 1869−1878.
(21) Cappelaere, E.; Cressely, R. *Colloid Polym. Sci.* **1997**, *275* (5), 407−418.
(22) Decruppe, J. P.; Cappelaere, E.; Cressely, R. *J. Phys. II* **1997**, *7* (2), 257−270.
(23) Cappelaere, E.; Cressely, R.; Decruppe, J. P. *Colloids Surf. A* **1995**, *104* (2/3), 353−74.
(24) Hartmann, V.; Cressely, R. *J. Phys. II* **1997**, *7* (8), 1087−1098.
(25) Kadoma, I. A.; Ylitalo, C.; Van Egmond, J. W. *Rheol. Acta* **1997**, *36* (1), 1−12.
(26) Marques, C. M.; Cates, M. E. *J. Phys. (Paris)* **1990**, *51* (16), 1733−1747.
(27) See, H.; Doi, M.; Larson, R. *J. Chem. Phys*. **1990**, *92*, 792−800.
(28) Boltenhagen, P.; Hu, Y.; Matthys, E. F.; Pine, D. J. *Europhys. Lett*. **1997**, *38* (5), 389−394.
(29) Penfold, J.; Staples, E.; Tucker, I.; Fragnetto, G. *Physica B (Amsterdam)* **1996**, *221* (1−4), 325−330.
(30) Bruinsma, R.; Gelbart, W.; Ben-Shaul, A. *J. Chem. Phys.* **1992**, *96*, 7710−7727.
(31) Wang, S.-Q. *J. Phys. Chem.* **1990**, *94* (22), 8381−8348.
(32) Wang, S.-Q.; Huang, F. Y. *Macromolecules* **1991**, *24* (10), 3004−3009. Wang, S.-Q. *Macromolecules* **1992**, *25* (3), 1153−1156.
(33) Wang, S.-Q. *Colloid Polym. Sci.* **1992**, *270*, 1130−1134.
(34) Cates, M. E.; Turner, M. S. *Europhys. Lett*. **1990**, *11* (7), 681−686.
(35) Cates, M. E.; Turner, M. S. *J. Phys.: Condens. Matter* **1992**, *4*, 3719−3741.
(36) Pilsl, H.; Hoffmann, H.; Hofmann, S.; Kalus, J.; Kencono, A. W.; Lindner, P.; Ulbricht, W. *J. Phys. Chem.* **1993**, *97*, 2745−2754.
(37) Hofmann, S.; Hoffmann, H.; Rauscher, A. *Ber. Bunsen-Ges. Phys. Chem.* **1991**, *95* (2), 153−164.
(38) Hofmann, S. Ph.D. Thesis, 1994, University of Bayreuth.
(39) Angel, H.; Hoffmann, H.; Krämer, U.; Thurn, H. *Ber. Bunsen-Ges. Phys. Chem*. **1989**, *93*, 184−191.
(40) Hoffmann, H.; Krämer, U.; Thurn, H. *J. Phys. Chem.* **1990**, *94*, 2027−2033.
(41) Walther, K.-L.; Krämer, U.; Hoffmann, H.; Wokaun, A. *Chem. Phys. Lett*. **1993**, *212*, 96−102.
(42) Thurston, G. B.; Bowling, D. I. *J. Colloid Interface Sci.* **1969**, 34.
(43) Cates, M. E. *J. Phys. II* **1992**, *2* (5), 1109−1119.
(44) Krämer, U. Ph.D. Thesis, 1991, University of Bayreuth.
(45) Thunig, C.; Hofmann, S. Private communication, University of Bayreuth.
(46) Tamori, K.; Esumi, K.; Meguro, K.; Hoffmann, H. *J. Colloid Interface Sci.* **1991**, *147* (1), 33−45.
(47) Shinoda, K. *Colloidal Surfactants*; Academic Press: New York, London, 1963; p 106 and references cited therein.
(48) Oetter, G.; Hoffmann, H. Unpublished results.
(49) Hoffmann, H.; Hofmann, S.; Illner, J. C. *Prog. Colloid Polym. Sci* **1994**, *94*, 103−109.
(50) Kalus, J.; Hoffmann, H.; Chen, S.-H.; Lindner, P. *J. Phys. Chem.* **1989**, *93*, 4267−4276.
(51) Kalus, J.; Lindner, P.; Hoffmann, H.; Ibel, K.; Münch, Ch.; Sandner, J.; Schmelzer, U.; Selbach, J. *Physica B* **1991**, *174*, 164−169.
(52) Münch, Ch.; Hoffmann, H.; Kalus, J.; Ibel, K.; Neubauer, G.; Schmelzer, U. *J. Appl. Crystallogr*. **1991**, *24*, 740−746.
(53) Dewalt, L E.; Farkas, K. L.; Abel, C. L.; Kim, M. W.; Pfeiffer, D. G.; Ou-Yang, M. D. *ACS Symp. Ser*. **1995**, *547* (Flow-Induced Structure in Polymers), 253−272.